AJP

ISSN : 0971 - 3093

Vol 25, No 3, March, 2016

ASIAN JOURNAL OF PHYSICS

An International Research Journal

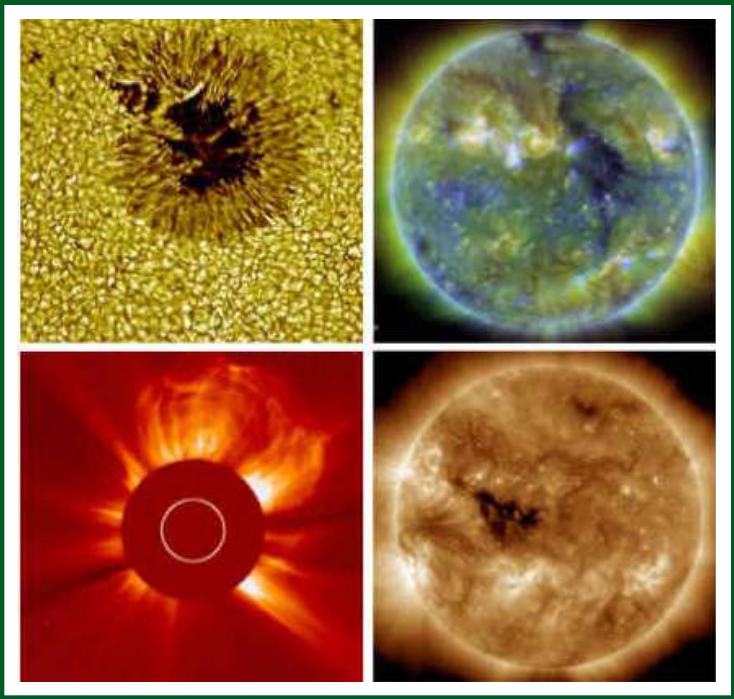

ANITA PUBLICATIONS

FF-43, 1st Floor, Mangal Bazar, Laxmi Nagar, Delhi-110 092, India

B O : 2, Pasha Court, Williamsville, New York-14221-1776, USA

ap

Asian Journal of Physics
Vol. 25, No 3 (2016) 325-340
Available on: www.asianjournalofphysics.in

Solar subsurface flows from local helioseismology

Junwei Zhao[1] and Ruizhu Chen[2,1]

[1]*W W Hansen Experimental Physics Laboratory, Stanford University, Stanford, CA 94305-4085, USA*
[2]*Department of Physics, Stanford University, Stanford, CA 94305-4060, USA*

In this article, we review recent progresses in subsurface flows obtained from two local helioseismology methods: time-distance helioseismology and ring-diagram analysis. We review results in the following four topics: flows beneath sunspots and active regions, supergranular subsurface flows, shallow meridional flow and its variations with solar cycles, and meridional circulation in the deep solar interior. Despite recent advancements in methodology, modeling, and observations, many questions are still to be answered and a few topics remain controversial. More efforts, especially in numerical modeling and accurate interpretation of acoustic wave travel-time measurements, are needed to improve the derivations of subsurface flows.

Keywords: Sun: seismology; Sun:interior; Sun: subsurface flows

1 Introduction

Solar subsurface flows concern the flow fields of convective flow cells (like supergranules and giant cells), sunspots and active regions on local scales, and zonal and meridional flows on global scales. These flows are believed to transport heat, magnetic flux, and angular momentum, helping to balance the Sun's convection and maintain its magnetic cycles. Studying these flows of different spatial scales is of great importance for us to understand the solar interior structures and dynamics, as well as its magnetic activities. Since these subsurface flows are hidden beneath the Sun's non-transparent surface and invisible to any direct observations, we rely on helioseismology, which studies the Sun's oscillation modes and propagating waves, to derive these otherwise undetectable properties. Indeed, the past two decades witnessed rapid advancements in understanding the Sun's interior structures and dynamics using observations from the *Global Oscillation Network Group* (*GONG*) [1], the *Solar and Heliospheric Observatory* / Michelson Doppler Imager (*SOHO*/MDI) [2], and the *Solar Dynamics Observatory* / Helioseismic and Magnetic Imager (*SDO*/HMI) [3, 4].

In this article, we categorize our review of subsurface flows into four topics: flows beneath sunspots and active regions, supergranular subsurface flows, shallow meridional flow and its temporal variations, and deep meridional-circulation profile. We hope the readers understand that this review is by far not a complete review covering all or most works related to these topics, but only those works we, the authors, are involved or familiar with. Meanwhile, we concentrate only on flows but not structures. For example, there were many works on sunspots' subsurface structures in the past 15 years or so, but we do not include those works in this review. Also, since rotation and torsional oscillation were reviewed by Howe [5] in this issue, in this article we focus on meridional circulation but exclude rotation-related works.

We think it is worth pointing out, at the beginning of this article, that all the four topics that we review are not uncontroversial. For example, how deep is a typical supergranule and what is its flow structure? How many meridional-circulation cells does the Sun have, in both its radial and latitudinal directions? There are no consensus answers to these questions. These nevertheless highlight that despite the great advancements

Corresponding author :
e-mail: junwei@sun.Stanford.EDU (Junwei Zhao)

in recent years, we are still in an early stage to understand the Sun's interior, to interpret the oscillations and waves that we observe, and to relate these observations with the Sun's interior properties. More works are badly needed to advance our knowledge in these regards.

2 Subsurface flows in active regions

2.1 Results from time-distance helioseismology

Time-distance helioseismology is one of local helioseismology techniques to investigate solar interior structures and dynamics in local areas [6, 7]. Technically, time-distance helioseismology measures travel times of helioseismic waves, including both surface gravity waves (*f*-mode) and acoustic waves (*p*-mode), from one surface location to another by cross-correlating oscillation signals observed at these two surface locations. The *f*-mode waves only propagate horizontally within the first 2 Mm beneath the photosphere, and are relatively easier to be utilized to study shallow horizontal flows [8, 9]. The *p*-mode waves penetrate into the solar interior, and the travel times that time-distance method measures are what it takes for waves to travel from one surface location to the other through a curved path in the solar interior. These acoustic waves carry the information of structure and dynamics from the interior back to the surface, and in principle, the measured travel times can be inverted for subsurface sound-speed perturbation and flow fields [10].

Inferring subsurface flows of sunspots or active regions is a primary investigation topic of time-distance helioseismology. Based on acoustic travel-time measurements, Duvall *et al* [7] reported detection of downdrafts beneath sunspots' surface, supporting Parker's cluster sunspot model [11]. Later, Kosovichev [10] developed an algorithm to invert these measurements for the sunspot's subsurface flow fields, and his inversion results showed converging and downward flows in the shallow regions, supporting Duvall *et al*'s claim [7]. These flows were believed to play a role in holding sunspots together from dissolving due to the magnetic repelling force. With the availability of higher-resolution observations from space-based instruments like *SOHO*/MDI [2], *Hinode*/SOT [12, 13], and *SDO*/HMI [3, 4], similar analyses were also performed to invert for subsurface flows in sunspots and active regions. Using MDI-observed *p*-mode waves, Zhao *et al* [14] found converging flows with a speed of about 500 ms^{-1} around the sunspot from surface to about 5 Mm in depth, and this converging flow was associated with a downward flow with a similar speed. On the other hand, this converging and downward flow pattern located in the same region where negative sound-speed perturbation was found [15]. Theoretically, this could be understood as cool materials near the surface of sunspots moved downward due to the higher density. Later analyses using *Hinode* and HMI data gave similar results [16, 17], which was expected because the analysis procedures were roughly the same. Using *f*-mode waves, Gizon *et al* [9, 18] reported outflows from sunspots (or moat flow) from the surface to about 2 Mm in depth. These results did not immediately reconcile with those reported by *p*-mode analysis, and how to understand these discrepancies has been long debated.

Sunspots' subsurface wave-speed perturbation is a controversial topic [18, 19] that we do not review in this article. And, whether the measured *p*-mode travel-time asymmetry in opposite traveling directions can be interpreted as caused by flows, like what helioseismologists usually do for quiet regions, is another controversial problem. Woodard [20] argued that wave absorption by sunspots could mimic the effect of travel-time anomaly, which might be mistakenly interpreted as flows. Lindsey & Braun [21, 22] demonstrated that the shower-glass effect, which smears the phases of incoming and outgoing acoustic waves, should be corrected before the travel-time measurements were inverted for flows, although how to correct this effect is a puzzling question. Some more recent analyses [23, 24] showed that the Wilson depression in sunspots also effected the interpretation of measured travel-times of acoustic waves. All these effects, caused by wave absorption, presence of magnetic field, atmospheric height depression, and maybe others, truly complicate the interpretation and inversion of helioseismic measurements, but how to effectively and accurately incorporate these effects in measurement and inversion processes remains a difficulty to be overcome by future studies.

Meanwhile, attempts have been made to analyze numerical simulations of sunspots to assess the time-distance analysis processes. Analyzing a realistic simulation of a sunspot model [25] using a local helioseismic method, Braun *et al* [26] found that their travel-time measurements were remarkably similar to those from observed sunspots, but these travel-time shifts were not expected from the flow fields in the model, questioning the basic philosophy of inverting travel times for flows in these areas. They argued that a new inversion method is needed for subsurface flows in magnetic regions. More recently, DeGrave *et al* [27] inverted travel-time measurements from realistic simulations of a sunspot and a pore for subsurface flow fields, and compared these inversion results with flows in the models. They found that they could recover the horizontal flows but underestimated the amplitude of flows by about 50%; however, they also found that they could not recover the vertical flows in these models. Nevertheless, this is a positive advancement toward a possible solution to the difficult obstacles of deriving sunspots' subsurface flows.

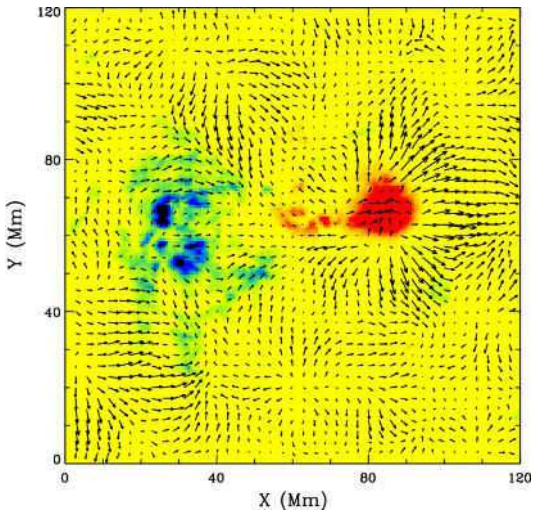

Fig 1. Example of subsurface flows at the depth of 0 – 1 Mm from HMI time-distance data-analysis pipeline, showing divergent flows in supergranules, converging flows inside a sunspot and outflows around it. The longest arrow represents a speed of 300 ms^{-1}. Background image shows the magnetic field of the region. Adapted from Ref [17] with permission.

Additional efforts were made to examine the accuracy of the helioseismically inverted flows by comparing them with the flows derived by tracking magnetic features on the surface. Liu *et al* [28] compared near-surface flows from the HMI time-distance pipeline [17] with the surface flows obtained from DAVE4VM, a method of tracking vector magnetic field and solving magnetic induction equations [29]. Their results showed a very good agreement in the vicinity of a simple sunspot, but in the sunspot's umbra, the subsurface flows were greater than the surface flows. This could be an underestimate of the surface flow speed in the umbra by the tracking method due to the umbra's featureless property, or due to that the strong magnetic field complicated the inversion of the time-distance measured travel times, as already introduced above. Although this comparison showed an encouraging sign of the validity of sunspots' subsurface flows, more works are nevertheless needed to address various effects in the magnetic regions.

2.2 Results from ring-diagram analysis

Ring-diagram analysis is another local helioseismology technique that analyzes oscillation modes of the Sun, just as global helioseismology does but for local areas [30]. The positions of oscillation modes can be precisely determined by fitting the power ridges in k-ω diagram, and the modes' position shifts can be

related to the subsurface structures and flow fields, which in principle can be inverted from the mode-position shift measurements. For a more detailed introduction of the methodology, one can refer to a recent article by Baldner *et al* [31].

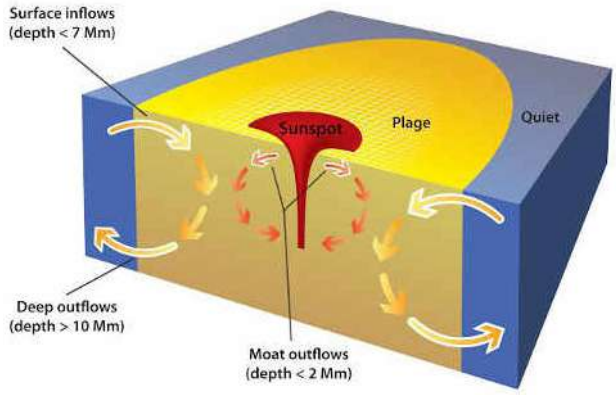

Fig 2. Schematic plot showing a side view of large-scale mass circulations based on high- and low-resolution ring-diagram analysis as well as local correlation tracking results. Adapted from Ref [34] with permission from AAS.

Because one needs a certain region to construct the k-ω diagrams and fit for the mode positions, this technique can only have a relatively poor spatial resolution, typically no better than 5°. Therefore, most results from ring-diagram analysis give relatively large-scale flow patterns around active regions. Haber *et al* [32] found a horizontal converging flow toward large active regions from the surface to a depth of at least 7 Mm, and a divergent flow from the active regions at and beneath at least 14 Mm. This flow pattern is similar to the large-scale flow pattern near large active regions obtained by the time-distance analysis [33]. Later, Hindman *et al* [34] further developed the ring-diagram analysis method into a high-resolution method, improving its resolution to 2°. Armed with the new method, they studied the material circulations around active regions, and found that almost all active regions possessed a mean inflow of 20-30 ms^{-1} and a cyclonic circulation of ~5 ms^{-1} at their peripheries. Near the cores of the active regions were zones of strong anti-cyclonic outflow with a speed of about 50 ms^{-1}. Figure 2 shows a schematic plot of the circulation structure they found.

Collective properties of some specific types of active regions, such as emerging regions, decaying regions, rotating sunspots, were also statistically studied. Komm *et al* [35] found that the average vertical flows, determined from horizontal flows with a combination of the mass-conservation equation, were mostly upward for emerging regions compared to the grand average of a large sample of regions. The vertical flows were more pronouncedly downward for decaying regions, especially near the depth of 8 Mm. Similar results were reported in follow-up studies [36, 37]. Through studying a few selected rotating sunspots, Jain *et al* [38] found that the subsurface flows associated with the rotating sunspots varied significantly with depths during the course of rotation, while the flow variations of non-rotating sunspots were primarily constant.

Validating subsurface flows derived from ring-diagram analysis using numerical simulation data, like what have been done for time-distance analyses [26, 27], were largely missing due to that no realistic numerical simulation has been made in a large enough region to carry out these analyses. Another approach, comparing ring-diagram derived near-surface flows with correlation tracking method on surface, like what Liu *et al* [28] did for time-distance analysis, was recently carried out by Jain *et al* [39]. An example of their results is illustrated in Fig 3. They found a positive correlation between flows derived from the ring-diagram

and local correlation tracking, implying that despite the absorption of acoustic power in magnetic regions, the flows inferred from the helioseismic analysis were still comparable to the surface measurements. However, they also cautioned that the helioseismically derived flows were about as twice large as the flows from the tracking method, the reason of which was not understood.

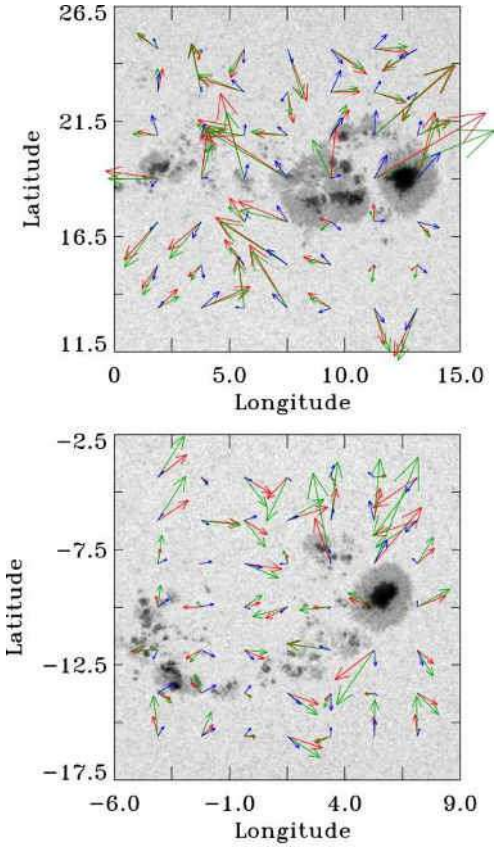

Fig 3. Comparison of horizontal flows: photospheric from local correlation tracking (blue), subphotospheric from *f*-modes (green), and subphotospheric from inverted *p*-modes measurements (red) in active regions NOAA 11339 (top) and 11890 (bottom). Adapted from Ref [39] with permission from AAS.

2.3 Subsurface properties and flaring activities

Whether the subsurface flows in and around active regions are related to, or even are able to be used to forecast, solar eruptive events is another interesting topic that some helioseismologists have explored. In principle, since helioseismology is able to provide three-dimensional subsurface flow fields, it is possible to calculate the distributions of subsurface vorticity and kinetic helicity, and try to relate these quantities with flaring activities.

Through analyzing a number of selected active regions, Komm *et al* [40] first reported that the maximum values of unsigned kinetic helicity density of each active region correlated remarkably well with the total flaring X-ray flux, and active regions with strong flaring activities showed large values of subsurface kinetic helicity density. With a larger sample of active regions, Mason *et al* [41] analyzed the relations between subsurface vorticity and flares. They reported that the horizontal components of vorticity were

correlated with the total flare intensity of corresponding active regions, and the vorticity was proportional to the product of total flare intensity and maximum unsigned magnetic flux. Similar studies with more samples were carried out later [42, 43]. By combining different subsurface quantities of active regions derived from ring-diagram analysis, Reinard *et al* [44] defined a parameter that seemed to be able to provide an advanced notice of flare occurrences (as shown in Fig 4), enhancing the hope of flare forecast.

Using subsurface flow fields from the HMI time-distance pipeline [17], Gao *et al* [45] studied connections between flares and subsurface properties with a higher spatial resolution and a higher temporal cadence. They found that the flare-prolific active regions often showed a bump in subsurface kinetic helicity before or during the occurrence of a major solar flare. A more systematic statistics with more flare samples in more active regions are needed to more convincingly establish a clear relationship between the subsurface properties with the flaring events.

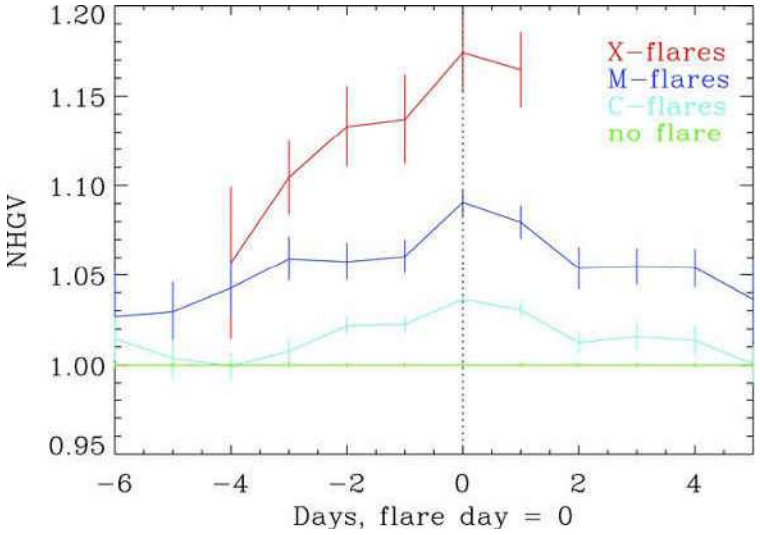

Fig 4. Superposed epoch analysis for the NHGV parameter of active regions associated with X- (red), M- (blue), and C-class (cyan) flares. The green line is an average value for active regions that do not flare. Adapted from Ref [44] with permission from AAS.

3 Subsurface flows of supergranules

Supergranulation was first found in 1950s [46], and has long been thought as medium-sized convection. These structures are often characterized by their association with magnetic networks [47] and divergent flows from the center of the structures [48]. Local helioseismology, particularly time-distance helioseismology, has been widely employed to study the subsurface flow fields of supergranules, to understand their horizontal and vertical flow patterns, as well as their depth extents. Although supergranules mostly locate in the Sun's quiet regions, where no strong magnetic fields are present to complicate the measurements and interpretation of helioseismic signals like in active regions, it turns out that the supergranular subsurface properties derived from the helioseismology technique are not controversy-free.

Duvall & Gizon [8] developed methods to measure supergranular flows using *f*-mode waves, and inversions were later carried out to derive the divergent flow fields in the near-surface depths [9]. These results were compared with local-correlation tracking results, and high similarities were found [49]. Using *p*-mode time-distance analysis, Zhao & Kosovichev [50] demonstrated that it was not difficult to invert the near-surface divergent flow patterns, but quite difficult to determine the vertical flow and to find the

converging flow in the deeper depths, which is expected from mass conservation if supergranules are truly convective cells. Since the divergent flow patterns and downflows contribute similarly to the measured acoustic travel-time shifts, known as cross-talk effect, it is difficult to disentangle these flows if not invoking other observational constraints [50]. Using a realistic simulation of solar convection [51], Zhao *et al* [52] demonstrated once again that the supergranular vertical flow was difficult to be reliably inverted due to its smaller amplitude and the cross-talk effect.

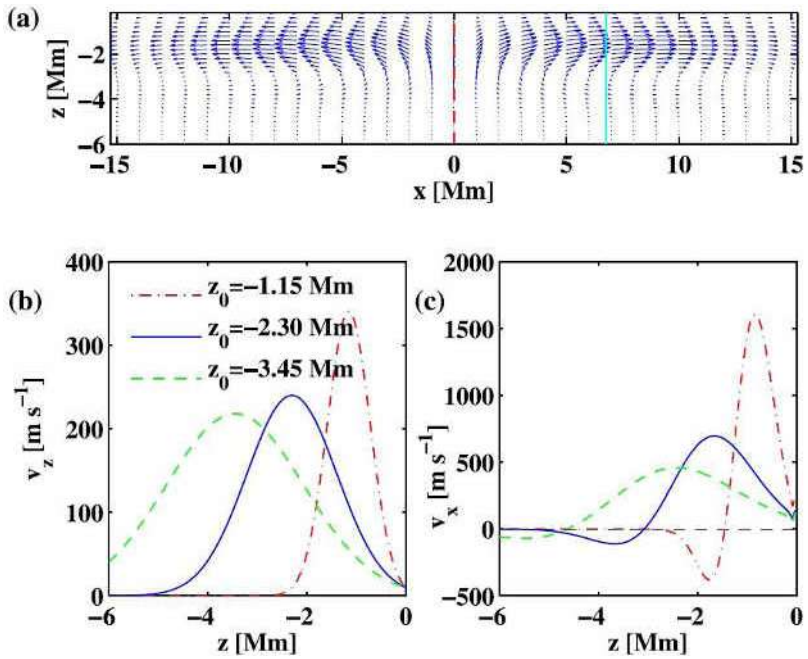

Fig 5. A supergranular model that satisfies time-distance measurements. (a) Velocity vectors with a peak upflow of 240 ms^{-1} at z = –2.3 Mm and a peak horizontal flow of 700 ms^{-1} at z = –1.6 Mm and x = 7 Mm. The blue lines in panels (b) and (c) are taken from the red dashed line and turquoise line in panel (a) and for vertical flow and horizontal flow, respectively. Other lines in (b) and (c) are taken from different models. Adapted from Ref [64] with permission from the authors.

Later, many authors have substantially improved their inversions by introducing wave-based sensitivity kernels and different inversion codes. For example, Jackiewicz *et al* [53] developed two-dimensional Fréchet kernels for the surface *f*-mode waves, Birch & Gizon [54] developed Born-approximation sensitivity kernels for 3-D vector subsurface flows, and Burston *et al* [55] computed 3-D Fréchet kernels for vector flows. These developments in principle could more accurately relate the subsurface flow fields with the measured helioseismic travel times on the surface. Regarding the inversion techniques, Jackiewicz *et al* [56] developed a high-resolution OLA inversion method for travel-time measurements, and they later further developed a three-dimensional SOLA inversion technique targeting for an inversion of 3-D subsurface flow vectors [57]. These developments led to a more reliable inversion of the supergranular subsurface flow with a more confident vertical flow in shallow layers [58]. The divergent flow pattern was more robustly inferred up to 3.5 Mm in depth, and the vertical flow was derived for the first 1 Mm after minimizing the cross-talk effect. However, despite these progresses, there are still a number of issues that weaken our confidence in the inverted supergranular subsurface flows, as recently pointed out by Švanda [59]. Among these issues, a puzzling one is that the inverted horizontal flows switch directions every a few megameters in depth,

prompting people to doubt the reliability of the inversion despite the progresses in inversion techniques and sensitivity-kernel calculations. That is, whether there are converging flow patterns beneath supergranular surface, confirming the convective nature of supergranulation, is still an open question.

Efforts have also been made to validate the analysis processes using numerical simulation data. Geogorbiani *et al* [60] analyzed realistic convection simulation data [51] using local correlation tracking and *f*-mode time-distance method, and reported that the near-surface flows from helioseismology were in very good agreement with the local correlation tracking results, as well as with the near-surface flow averaged from the model. Using same datasets, Zhao *et al* [52] reported that they could satisfactorily invert the horizontal flows up to about 4 Mm in depth, but could not recover vertical flows due to cross-talk effect, as already reviewed above. More recently, DeGrave *et al* [61] utilized a set of simulation in a larger box and analyzed by combining different types of Fourier-domain filters, and concluded that the flows could be well retrieved in the upper ~3 Mm of the box while the vertical flows, even near-surface, could be hardly recovered reliably.

What is more controversial is the depth of supergranulation. Earlier Dopplergram observation and local correlation tracking method gave a prediction of the supergranular flow no deeper than 2.4 Mm in depth [48]. Based on early time-distance inversion results on supergranular flows, Duvall [62] estimated a supergranulation depth of about 8 Mm, while Zhao & Kosovichev [50] estimated the depth to be about 15 Mm using another set of flow inversion results. However, more recently, through a combination of time-distance measurements and forward modeling, Duvall & Hanasoge [63] argued that supergranulation is a shallow phenomenon with a depth of 2.3 Mm, in rough agreement with earlier result in 1990s [48]. They also reported a peak upward flow of 240 ms^{-1} at a depth of 2.3 Mm and a peak horizontal flow of 700 ms^{-1} at a depth of 1.6 Mm. Later, Duvall *et al* [64] further examined the simulation data made using their favored supergranular model, and found that new measurements from simulations supported their previous report of shallow supergranulation. Figure 5 shows a picture of their favored model for the supergranular subsurface flows. However, on the other hand, Hathaway [65] found that even at depths of ~50 Mm, he was still able to detect the flows associated with surface supergranules. How deep supergranules are seems to be a question that will haunt for a while.

4 Shallow meridional flow and its temporal variations

Both the internal rotation and meridional flow are favorite research topics of helioseismology. As reviewed by Howe [5] in this issue, solar internal rotation does not stay stationary but changes with the phase of solar cycles, known as torsional oscillation [66, 67]. The torsional oscillation has two branches, one drifting toward the pole and one migrating toward the equator together with the activity belts. The lower branch of the torsional oscillation exhibits as faster and slower zonal-flow bands, residing on both sides of the activity belts. This phenomenon was first studied using global helioseismology analysis, but was later widely studied by both ring-diagram [e.g., 68, 69, 70] and time-distance analysis techniques [e.g., 33, 71].

Meridional flow is mainly poleward on the surface and in shallow depths, and this was already well recognized in earlier helioseismic studies. By use of time-distance helioseismology, Giles *et al* [72] for the first time reported a poleward meridional flow from the surface up to 0.97 R_{SUN} in depth with a speed of ~20 ms^{-1}. Using ring-diagram analysis, González Hernández *et al* [73] also reported similar results. Since then, poleward flow with a speed of about 20 ms^{-1} was widely agreed by many follow-up works in the depths no deeper than about 30 Mm.

Meanwhile, temporal variations of the meridional flow became another favorite topic by local helioseismologists. For deeper regions, using time-distance measurements, Chou *et al* [74] reported that in addition to the poleward flow, the meridional flow had an extra component of diverging flows from the active zones up to 77 Mm below the solar surface. Later analysis by Beck *et al* [75] covering a longer period using

nearly continuous data confirmed these results. Both these works focused on longer acoustic travel distances, i.e., deeper interior, and did not invert the travel-time measurements for meridional-flow speed. However, a more recent analysis in 2015 argued that the surface magnetic field might have contaminated the measured travel times in this type of measurements, and caused these extra components that were actually not there [76]. After getting rid of the magnetic-field effect, Liang & Chou [77] found a change of meridional-flow speed of about 10 ms^{-1} around the bottom of the convection zone from solar minimum to solar maximum years.

There are more works concerning the temporal evolution of meridional flow in the depths shallower than 30 Mm. By use of dense-pack ring-diagram analysis, Haber *et al* [78] analyzed organized flow patterns in the upper convection zone, and in a later paper [68], they reported that with the evolution of the solar cycle toward the maximum, the gradient of meridional flow near the equator deepened. They also reported extra meridional-circulation cells merging and submerging in higher latitude, but this phenomenon was later dismissed as an effect caused by the variation of solar B-angle [79]. Using a similar analysis procedure, Basu & Antia [69] reported that the meridional flow showed distinct activity-related changes, and the anti-symmetric component of the meridional flow showed a decrease in speed with the magnetic activity.

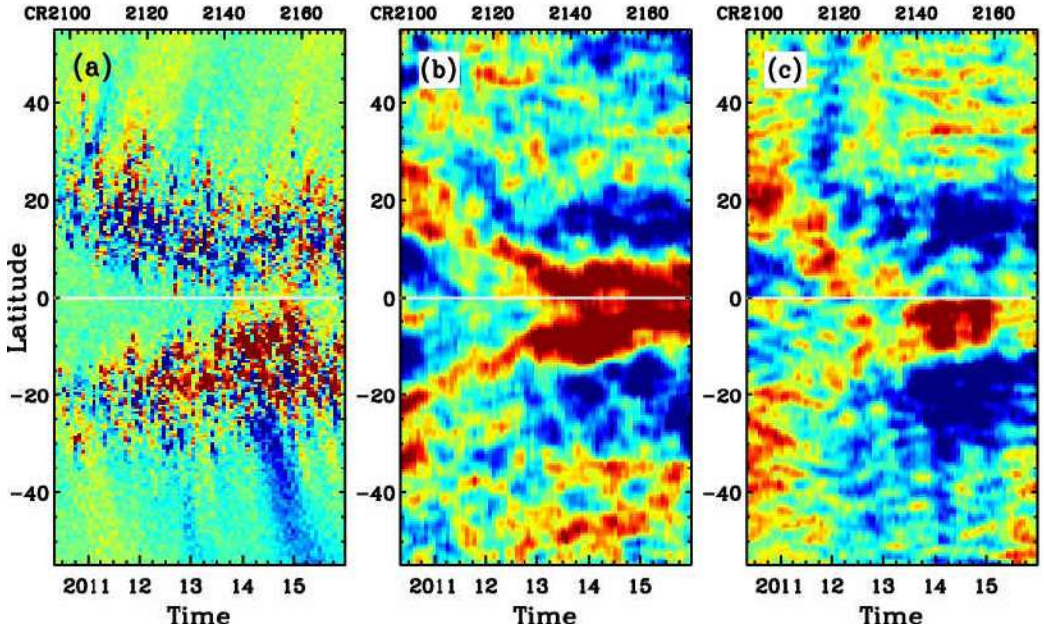

Fig 6. (a) Butterfly diagram for magnetic field between 2010 May and 2015 December, observed by HMI. (b) Zonal flow (rotational profiles after a long-time mean is subtracted) during the same period. Red (blue) represents faster (slower) flow than the mean, and color scale is between –5 and 5 ms^{-1}. (c) Residual meridional flow (meridional flow profiles after a long-time mean is subtracted) for the same period. Red (blue) represents poleward (equatorward) flow, and color scale is between –7 and 7 ms^{-1}. This plot is based on Ref. [71] but with a longer analysis period.

Using time-distance method, Zhao & Kosovichev [33] investigated variations of the meridional flow with time by subtracting a solar minimum-year meridional-flow profile from all other years. They found the residual meridional flow showed a converging-flow pattern toward the activity belts in both hemispheres. They suggested that this converging flow was due to the downdrafts of cool materials in the activity zones, as proposed by Spruit [80]. This flow pattern was also studied by Gizon [81] and González Hernández *et al* [82],

among others. Later, González Hernández *et al* [83] reported that the converging flow pattern also extended into the solar minimum years when there was little magnetic activity, indicating that the flow pattern might not be an artifact caused by the magnetic field. Through tracking motions of surface magnetic elements, Hathaway & Rightmire [84] also found similar flow patterns, and this was an independent confirmation of these results using a non-helioseismic method. By combining observational analysis and numerical modeling, Gizon & Rempel [85] suggested that the additional meridional-flow component was likely a geostrophic flow caused by the increased radiative loss in the activity belts. Figure 6 shows recent results of torsional oscillation (or zonal flow) and residual meridional flow obtained by the HMI time-distance pipeline [71].

In addition to the study on the meridional-flow pattern around activity belts, there were also other works studying the differences in meridional-flow speeds during the solar activity maximum and minimum. Hathaway & Rightmire [86] studied the advection of magnetic field and determined the meridional-flow speed covering the entire cycle 23. They found that the meridional-flow speed was faster in activity minimum years than in maximum years, and was substantially faster in the minimum approaching cycle 24 than the corresponding minimum approaching cycle 23. They related the increase of the meridional-flow speed to the extended minimum after cycle 23. Basu & Antia [87] also reported the similar trend that the meridional-flow speed was faster during activity minimum years than the maximum years. More recent studies reported that the same trend continued into the current solar cycle [71, 88].

Whether there are extra circulation cells in high-latitude areas is another interesting question that many authors have investigated. For surface measurements using HMI magnetic field data, Rightmire-Upton *et al* [89] reported that the poleward meridional flow extended at least to 5° within the pole, and did not find evidences of counter-flow cells above that. Using ring-diagram analysis, Komm *et al* [90] found that the poleward flow at various depths at least extended to 75°. Although during some periods a counter-flow cell was detected, that was more likely due to the effect of solar B-angle and could not be trusted. However, using a global helioseismology method, Schad *et al* [91] reported a multi-cell structure in both latitudinal and radial directions, suggesting a high-latitude counter-flow cell. Therefore, whether there is a counter-flow cell residing in the Sun's high-latitude area, it is still an open question that demands more work, and probably off-ecliptic observations that rely on future space missions.

A more recent study [71], focusing on the temporal evolution of meridional flow during the rising phase of the solar cycle 24 using HMI data, reported an interesting anti-correlation between the meridional-flow speed and the magnetic flux in the mid-latitude areas. It was found that the meridional-flow speed slowed down when the following-polarity magnetic flux was transported to cancel the existing magnetic field in the polar region, and the flow sped up when the leading-polarity flux was transported poleward to enhance the existing magnetic field in the polar region. It is unclear why the flow speed is coupled with the magnetic flux this way, but this interesting phenomenon certainly has an interesting implication to the polarity reversal in the polar region [92].

5 Deep meridional circulation

The global-scale meridional circulation is crucial for understanding solar dynamics and solar cycles, and plays an important role in transporting magnetic flux and redistributing angular momentum [93]. Despite the facts that the internal rotational profile has been long established and the shallow meridional flow was widely studied, the deep meridional-circulation profile is much more difficult to detect and remains an active topic being studied by different groups using various approaches.

As already mentioned in Sec. 4, the meridional flow on the surface and in shallow interior were reliably determined as poleward with a speed of about 20 ms^{-1}, but the returning equatorward flow, expected to be inside the Sun so as to balance the poleward flow and keep mass conserved, was not reliably detected

for a long time. Giles [94] inverted his long-distance travel-time measurements, but found poleward flows through the entire convection zone. After invoking mass-conservation constraint, he reported a 2 ms^{-1} return flow near the bottom of the convection zone. For many years after that, a single-cell meridional-circulation model with a deep equatorward flow was widely believed in the solar physics community, and this model helped the development of flux-transport solar dynamo model [95].

In 2007, Mitra-Kraev & Thompson [96] used a method pioneered by Braun & Fan [97], measured frequency shifts of solar oscillations due to the north-south directed meridional flow, and inverted these measurements for flows. They reported an equatorward flow at the depth of about 50 Mm, but their measurement errors were large. In 2012, by tracking the supergranular patterns observed by MDI, Hathaway [98] found a significant equatorward flow (4.6±0.4 ms^{-1}) at a depth of ~70 Mm (or 0.90 R_{SUN}). However, the determination of the depth of flows from this method was tricky, and he tried to match the rotational properties of supergranules with the differential rotation inferred by global helioseismology. The physical reasoning behind this is unclear, and this leads to some suspicions in these results.

On the other hand, the discovery of a systematic center-to-limb effect in helioseismic measurements allowed a more robust inference of the deep meridional flow. The systematic center-to-limb effect in time-distance method exhibits as an extra travel-time shift, as a function of disk location and measurement distance, and this effect must be removed from travel-time measurements before inversion is done [99].

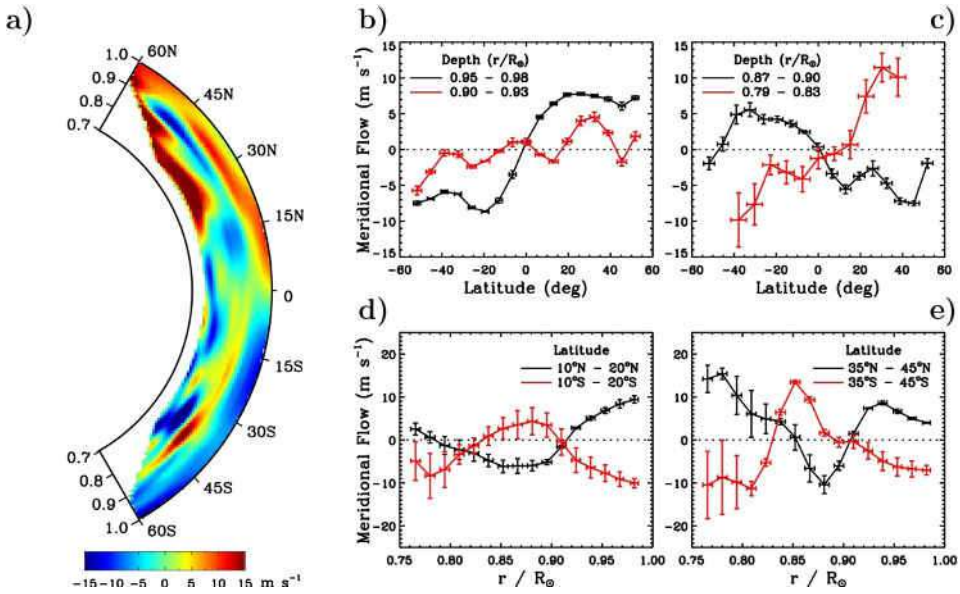

Fig 7. Meridional-flow profile obtained from time-distance inversion. Panel (a) shows a cross-sectional view of the meridional circulation, with positive velocity directing northward. Panels (b) and (c) show the inverted velocity as functions of latitude averaged over some depths. Panels (d) and (e) show the velocity as a function of depth averaged over some latitudinal bands. Adapted from Ref [100] with permission from AAS.

Using the first two years' continuous HMI observations and after removing the systematic effect, Zhao *et al* [100] reported a double-cell circulation, with a 15 ms^{-1} poleward flow from the surface to about 0.91 R_{SUN} and a 10 ms^{-1} equatorward extending from 0.91R_{SUN} to 0.82 R_{SUN}. The flow direction turned to poleward again below that and persisted to at least 0.75R_{SUN} or so. Figure 7 displays their meridional circulation results. Later, Kholikov *et al* [101] and Jackiewicz *et al* [102] measured and inverted two years

of GONG data following the same measuring and systematic-effect-correcting strategies prescribed by Zhao *et al* [100]. The results from these two different instruments agreed well in the outer 15% of solar radius, i.e., a shallow equatorward flow and the depth of flow turn-over, but were at odds in the deeper interior. More recently, Rajaguru & Antia [103] also carried out time-distance measurements using the HMI data, and performed inversions after including the mass-conservation equation and the radial flow component, both of which were not included in the previous studies. They reported a single-cell circulation and a deep equatorward flow beneath 0.77 R_{SUN}, not much different from the early circulation model by Giles [94]. What is truly the profile of the meridional circulation is still not yet within our touch.

Another approach to probe the meridional-circulation structure is to use global helioseismology, a method developed in recent years by Schad *et al* [104]. The meridional flow as a perturbation distorts the p-mode oscillation eigenfunctions, represented by mixing of unperturbed modes. The amplitude ratios of such mixed modes in Fourier domain, measurable using global oscillation data, are quantitatively related to meridional flow and in principle can be inverted for meridional flow. The measuring and inversion were done by Schad *et al* [91] using MDI 2004-2010 Dopplergram data. Their results showed evidence of a non-zero meridional flow at the base of the convection zone, and the meridional-circulation profile between 0.82 to 0.97 R_{SUN} exhibited multiple-cell structures in both latitude and depth. The general picture from this approach has both similarities and discrepancies comparing with that from the time-distance helioseismology, and a more detailed comparison among all the above-mentioned results and methods will help to progress toward a better determination of the solar meridional-circulation profile.

6 Discussions

We have reviewed progresses obtained by local helioseismology methods in subsurface flows of sunspots and active regions, subsurface supergranular flows, shallow meridional flow, and deep meridional circulation. As we can see, despite the rapid progresses in data acquisition, numerical modeling, and inversion techniques, many topics still remain largely controversial and confusing.

Regarding sunspots and active regions, although converging and downward flows were reported in earlier studies, some effects due to Wilson depression, influence of magnetic field, and complex spectrum-line formation above sunspots, all make the interpretation of the measured acoustic travel times very difficult if possible at all.

Regarding subsurface flows beneath supergranules, although there is no effect due to magnetic field, the inversion of vertical flows and the search for converging return flows continue puzzling many helioseismologists. In spite of recent reports of shallow depths of supergranules, others still believe that supergranules penetrate into very deep interior. The only consensus seems to be that the divergent flows persist from the surface to at least 3 or 4 Mm in depth.

Regarding shallow meridional flow, the converging flow pattern toward the activity belts in residual meridional flow is a well-agreed phenomenon by many different analysis methods. And many agree that there is no counter-flow cell at least lower than 75° latitude on the surface and in the shallow interior.

Regarding deep meridional-circulation profile, two questions need definite answers: how many circulation cells are there in the radial direction, and at what depth does the poleward flow switch direction to equatorward? Although the three papers published in 2012 and 2013 within one year span [98, 100, 91] all pointed to double- or multi-cell circulation and a shallow equatorward flow near 65 Mm in depth, a recent publication [103] suggested a single-cell circulation with a deep equatorward flow.

To solve some of these obstacles, we believe it is important to do more studies in realistic simulations, on both local and global scales and for both magnetized and non-magnetized models. Moreover, more careful works are needed in modeling the spectrum-line formation in the solar atmosphere, because a slight different

atmospheric height may give us quite different phase shifts in acoustic waves. How do wave phases behave in the atmosphere above the height of frequency cut-off? This also has important implications in interpreting the measured acoustic travel times. Clearly, there are many unanswered questions in local helioseismology, and the derivation of subsurface flows requires more efforts from more scientists.

Acknowledgments

J Z is partly supported by a NASA Grant NNX15AL64G, and R C is partly supported by the NASA Earth and Space Science Fellowship.

References

1. Arvey J W, Hill F, Hubbard R, Kennedy J R, Leibacher J W, Pintar J A, Gilman P A, Noyes R W, Title A M, Toomre J, Ulrich R K, Bhatnagar A, Kennewell J A, Marquette W, Patron J, Saa O, Yasukawa E, *Science*, 272 (1996)1284-1286.
2. Scherrer P H, Bogart R S, Bush R I, Hoeksema J T, Kosovichev A G, Schou J, Rosenberg W, Springer L, Tarbell T D, Title A, Wolfson C J, Zayer I, MDI Engineering Team, *Sol Phys*, 162(1995)129-188.
3. Scherrer P H, Schou J, Bush R I, Kosovichev A G, Bogart R S, Hoeksema J T, Liu Y, Duvall T L, Zhao J, Title A M, Schrijver C J, Tarbell T D, Tomczyk S, *Sol Phys*, 275(2012)207-227.
4. Schou J, Scherrer P H, Bush R I, Wachter R, Couvidat S, Rabello-Soares M C, Bogart R S, Hoeksema J T, Liu Y, Duvall T L, Akin D J, Allard B A, Miles J W, Rairden R, Shine R A, Tarbell T D, Title A M, Wolfson C J, Elmore D F, Norton A A, Tomczyk S, *Sol Phys*, 275(2012)229-259.
5. Howe R, *Asian J Phys*, 25(2016)311-324.
6. Duvall T L (Jr), Jefferies S M, Harvey J W, Pomerantz M A, *Nature*, 362(1993)430-432.
7. Duvall T L, D'Silva S, Jefferies S M, Harvey J W, Schou J, *Nature*, 379(1996)235-237.
8. Duvall T L (Jr), Gizon, L, *Sol Phys*, 192(2000)177-191.
9. Gizon L, Duvall T L (Jr), Larsen R M, *J Astrophys Astron*, 21(2000)339.
10. Kosovichev A G, *Astrophys J*, 461(1996)L55.
11. Parker E N, *Astrophys J*, 230(1979)905-923.
12. Tsuneta S, Ichimoto K, Katsukawa Y, Nagata S, Otsubo M, Shimizu T, Suematsu Y, Nakagiri M, Noguchi M, Tarbell T, Title A, Shine R, Rosenberg W, Hoffmann C, Jurcevich B, Kushner G, Levay M, Lites B, Elmore D, Matsushita T, Kawaguchi N, Saito H, Mikami I, Hill L D, Owens J K, *Sol Phys*, 249(2008)167-196.
13. Sekii T, Kosovichev A G, Zhao J, Tsuneta S, Shibahashi H, Berger T E, Ichimoto K, Katsukawa Y, Lites B, Nagata S, Shimizu T Shine R A Suematsu Y, Tarbell T D, Title A M, *Publ Astron Soc Japan*, 59(2007)S637-S641.
14. Zhao J, Kosovichev A G, Duvall T L (Jr), *Astrophys J*, 557(2001)384-388.
15. Kosovichev A G, Duvall T L (Jr), Scherrer P H, *Sol Phys*, 192(2000)159-176.
16. Zhao J, Kosovichev A G, Sekii T, *Astrophys J*, 708(2010)304-313.
17. Zhao J, Couvidat S, Bogart R S, Parchevsky K V, Birch A C, Duvall T L (Jr), Beck J G, Kosovichev A G, Scherrer P H, *Sol Phys*, 275(2012)375-390.
18. Gizon L, Schunker H, Baldner C S, Basu S, Birch A C, Bogart R S, Braun D C, Cameron R, Hanasoge S M, Jackiewicz J, Roth M, Stahn T, Thompson M J, Zharkov S, *Space Sci Rev*, 144(2009)249-273.
19. Kosovichev A G, Basu S, Bogart R, Duvall T L (Jr), González Hernández I, Haber D, Hartlep, T, Howe R, Komm R, Kholikov S, Parchevsky K V, Tripathy S, Zhao J, *J Phys Conf Ser*, 271(2011)012005.
20. Woodard M F, *Astrophys J*, 485(1997)890-894.
21. Lindsey C, Braun D C, *Astrophys J*, 620(2005)1107-1117.
22. Lindsey C, Braun D C, *Astrophys J*, 620 (2005) 1118-1131.

23. Lindsey C, Cally P S, Rempel M, *Astrophys J*, 719(2010)1144-1156.
24. Schunker H, Gizon L, Cameron R H, Birch A C, *Astron Astrophys*, 558(2013)A130.
25. Rempel M, *Astrophys J*, 740(2011)15.
26. Braun D C, Birch A C, Rempel M, Duvall T L, *Astrophys J*, 774(2012)77.
27. DeGrave K, Jackiewicz J, Rempel M, *Astrophys J*, 794(2014)18.
28. Liu Y, Zhao J, Schuck P W, *Sol Phys*, 287(2013)279-291.
29. Schuck P W, *Astrophys J*, 683(2008)1134-1152.
30. Hill F, *Astrophys J*, 333(1988)996-1013.
31. Baldner C S, Basu S, Bogart R S, Burtseva O, González Hernández I, Haber D, Hill F, Howe R, Jain K, Komm R, Rabello-Soares M C, Tripathy S, *Sol Phys*, 287(2013)57-69.
32. Haber D A, Hindman B W, Toomre J, Thompson M J, *Sol Phys*, 220(2004)371-380.
33. Zhao J, Kosovichev A G, *Astrophys J*, 603(2004)776-784.
34. Hindman B W, Haber D A, Toomre J, *Astrophys J*, 698(2009)1749-1760.
35. Komm R W, Howe R, Hill F, *Sol Phys*, 258(2009)13-30.
36. Komm R W, Howe R, Hill F, *Sol Phys*, 268(2011)407-428.
37. Komm R W, Howe R, Hill F, *Sol Phys*, 277(2012)205-226.
38. Jain K, Komm R W, González Hernández I, Tripathy S C, Hill F, *Sol Phys*, 279(2012)349-363.
39. Jain K, Tripathy S C, Ravindra B, Komm R, Hill F, *Astrophys J*, 816(2016)5.
40. Komm R, Howe R, Hill F, González Hernández I, Toner C, *Astrophys J*, 630(2005)1184-1193.
41. Mason D, Komm R, Hill F, Howe R, Haber D, Hindman B W, *Astrophys J*, 645(2006)1543-1553.
42. Komm R, Hill F, *J Geophys Res*, 114(2009)A06105.
43. Komm R, Ferguson R, Hill F, Barnes G, Leka K D, *Sol Phys*, 26(2011)389-406.
44. Reinard A A, Henthorn J, Komm R, Hill F, *Astrophys J*, 710(2010)L121-L125.
45. Gao Y, Zhao J, Zhang H, *Sol Phys*, 289(2014)493-502.
46. Hart A B, *Mon Not Royal Astron Soc*, 114(1954)17.
47. Simon G W, Leighton R B, *Astrophys J*, 140(1964)1120.
48. November L J, *Sol Phys*, 154(1994)1-17.
49. DeRosa M, Duvall T L (Jr), Toomre J, *Sol Phys*, 192(2000)351-361.
50. Zhao J, Kosovichev A G, in SOHO 12 / GONG+ 2002. Local and Global Helioseismology: the Present and Future, (ed) H Sawaya-Lacoste, ESA SP, 517(2003)417-420.
51. Benson D, Stein R, Nordlund Å, in Solar MHD Theory and Observations: A High Spatial Resolution Perspective, (eds) J Leibacher, R F Stein, H Uitenbroek, *Astron Soc Pacific Conf Se*r, 354(2006)92-96.
52. Zhao J, Georgobiani D, Kosovichev A G, Benson D, Stein R F, Nordlund Å, *Astrophys J*, 659(2007)848-857.
53. Jackiewicz J, Gizon L, Birch A C, Duvall T L (Jr), *Astrophys J*, 671(2007)1051-1064.
54. Birch A C, Gizon L, *Astron Nachr*, 32(2007)228.
55. Burston R, Gizon L, Birch A C, *Space Sci Rev*, 196(2015)201-219.
56. Jackiewicz J, Gizon L, Birch A C, *Sol Phys*, 251(2008)381-415.
57. Jackiewicz J, Birch A C, Gizon L, Hanasoge S M, Hohage T, Ruffio J-B, Švanda M, *Sol Phys*, 276(2012)19-33.
58. Švanda M, Gizon L, Hanasoge S M, Ustyugov S D, *Astron Astrophys*, 530(2011)A148.
59. Švanda M, *Astron Astrophys*, 575(2015)A122.
60. Georgobiani D, Zhao J, Kosovichev A G, Benson D, Stein R F, Nordlund Å, *Astrophys J*, 657(2007)1157-1161.
61. DeGrave K, Jackiewicz J, Rempel M, *Astrophys J*, 788(2014)127.

62. Duvall T L (Jr), in Structure and Dynamics of the Interior of the Sun and Sun-like Stars, (eds) S Korzennik, A Wilson, ESA SP, 418(1998)581-585.
63. Duvall T L, Hanasoge S M, *Sol Phys*, 287(2013)71-83.
64. Duvall T L, Hanasoge S M, Chakraborty S, *Sol Phys*, 289(2014)3421-3433.
65. Hathaway D H, *Astrophys J*, 749(2012)L13.
66. Howard R, LaBonte B J, *Astrophys J*, 239(1980)L33-L36.
67. Howe R, Christensen-Dalsgaard J, Hill F, Komm R W, Larsen R M, Schou J, Thompson M J, Toomre J, *Astrophys J Lett*, 533(2000)L163-L166.
68. Haber D A, Hindman B W, Toomre, J, Bogart R S, Larsen R M, Hill F, *Astrophys J*, 570(2002)855-864.
69. Basu S, Antia H M, *Astrophys J*, 585(2003)553-565.
70. Komm R, Howe R, Hill F, *Sol Phys*, 254(2009)1-15.
71. Zhao J, Kosovichev A G, Bogart R S, *Astrophys J Lett*, 789(2014)L7.
72. Giles P M, Duvall T L, Scherrer P H, Bogart R S, *Nature,* 390(1997)52-54.
73. González Hernández I, Patrón J, Bogart R S, the SOI Ring Diagram team, *Astrophys J Lett*, 510(1999)L153-L156.
74. Chou D -Y, Dai D -C, *Astrophys J*, 559(2001)L175-L178.
75. Beck J G, Gizon L, Duvall T L (Jr), *Astrophys J*, 575(2002)L47-L50.
76. Liang Z -C, Chou D-Y, *Astrophys J*, 805(2015)165.
77. Liang Z -C, Chou D-Y, *Astrophys J*, 809(2015)150.
78. Haber D A, Hindman B W, Toomre J, Bogart R S, Thompson M J, Hill F, *Sol Phys*, 192(2000)335-350.
79. González Hernández I, Komm R, Hill F, Howe R, Corbard T, Haber D A, *Astrophys J*, 638(2006)576-583.
80. Spruit H C, *Sol Phys*, 213(2003)1-21.
81. Gizon L, *Sol Phys*, 224(2005)217-228.
82. González Hernández I, Kholikov S, Hill F, Howe R, Komm R, *Sol Phys*, 252(2008)235-245.
83. González Hernández I, Howe R, Komm R, Hill F, *Astrophys J Lett*, 713(2010)L16-L20.
84. Hathaway D H, Rightmire L, *Astrophys J*, 729(2011)80.
85. Gizon L, Rempel M, *Sol Phys*, 251(2008)241-259.
86. Hathaway D H, Rightmire L, *Science*, 327(2010)1350.
87. Basu S, Antia H M, *Astrophys J*, 717 (2010) 488-495.
88. Komm R, González Hernández I, Howe R, Hill F, *Sol Phys*, 290(2015)3113-3136.
89. Rightmire-Upton L, Hathaway D H, Kosak K, *Astrophys J*, 761(2012)14.
90. Komm R, González Hernández I, Hill F, Bogart R, Rabello-Soares M C, Haber D, *Sol Phys*, 287(2013)85-106.
91. Schad A, Timmer J, Roth M, *Astrophys J lett*, 78(2013)L38.
92. Sun X, Hoeksema J T, Liu Y, Zhao J, *Astrophys J*, 798(2015)114.
93. Miesch M S, *Living Rev Sol Phys*, 2(2005)1.
94. Gile P M, Time-distance measurements of large-scale flows in the solar convection zone, Ph.D. Thesis, Stanford Univ, (1999).
95. Dikpati M, Charbonneau P, *Astrophys J*, 518(1999)508-520.
96. Mitra-Kraev U, Thompson M J, *Astron Nachr*, 328(2007)1009-1012.
97. Braun D C, Fan Y, *Astrophys J Lett*, 508(1998)L105-L108.
98. Hathaway D H, *Astrophys J*, 760(2012)84.
99. Zhao J, Nagashima K, Bogart R S, Kosovichev A G, Duvall T L (Jr), *Astrophys J*, 749(2012)L5.

100. Zhao J, Bogart R S, Kosovichev A G, Duvall T L (Jr), Hartlep T, *Astrophys J Lett*, 774(2013)L29.
101. Kholikov S, Serebryanskiy A, Jackiewicz J, *Astrophys J*, 784(2014)145.
102. Jackiewicz J, Serebryanskiy A, Kholikov S, *Astrophys J*, 805(2015)133.
103. Rajaguru S P, Antia H M, *Astrophys J*, 813(2015)114.
104. Schad A, Trimmer J, Roth M, *Astrophys J*, 734(2011)97.

[*Received*: 4.2.2016 ; *accepted*: 19.2.2016]